Electronic Structure and Properties of Transition Metal−Benzene Complexes

Ravindra Pandey,[†] Bijan K. Rao,*[,‡] Purusottam Jena,[‡] and Miguel Alvarez Blanco[§]

Contribution from the Physics Department, Michigan Technological University, Houghton, Michigan 49932, Physics Department, Virginia Commonwealth University, Richmond, Virginia 23284-2000, and Departamento de Quìmica Fìsica y Analìtica, Universidad de Oviedo, 33006-Oviedo, Spain

Received September 29, 2000. Revised Manuscript Received December 8, 2000

Abstract: A comprehensive theoretical study of the geometries, energetics, and electronic structure of neutral and charged 3d transition metal atoms (M) interacting with benzene molecules (Bz) is carried out using density functional theory and generalized gradient approximation for the exchange-correlation potential. The variation of the metal−benzene distances, dissociation energies, ionization potentials, electron affinities, and spin multiplicities across the 3d series in MBz complexes differs qualitatively from those in $M(Bz)_2$. For example, the stability of $Cr(Bz)_2$ is enhanced over that of CrBz by almost a factor of 30. On the other hand, the magnetic moment of $Cr(Bz)_2$ is completely quenched although CrBz has the highest magnetic moment, namely $6\mu_B$, in the 3d metal−benzene series. In multidecker complexes involving $V_2(Bz)_3$ and $Fe_2(Bz)_3$, the metal atoms are found to couple antiferromagnetically. In addition, their dissociation energies and ionization potentials are reduced from those in corresponding $M(Bz)_2$ complexes. All of these results agree well with available experimental data and demonstrate the important role the organic support can play on the properties of metal atoms/clusters.

I. Introduction

Studies of the chemistry of organometallic complexes[1,2] consisting of metal atoms, metal clusters, and metal surfaces interacting with organic molecules have been carried out for a long time using conventional chemical synthesis procedure. A fundamental understanding of this interaction, however, is hampered by the fact that one must incorporate the effects of the solvent. In the past decade, laser vaporization techniques have provided an alternate route to produce these complexes in the gas phase,[3−21] thus eliminating the need to invoke solvation effects. In this technique a laser beam vaporizes the target metal, and the ensuing hot plume of metal atoms is cooled in an inert gas environment seeded with the appropriate organic molecules. Analysis of their mass spectra, reactivity of mass selected species with reagent molecules, mobilities, ionization potentials (I.P.), and dissociation energies provide information on their atomic and electronic structure.

Considerable experimental effort[22] in this regard has been devoted to the study of 3d transition metal atoms (M = Sc, Ti, V, Cr, Mn, Fe, Co, Ni) interacting with benzene molecules (Bz). By varying the partial pressure of benzene and metal vapor as well as temperature, a large array of metal−benzene complexes have been produced and analyzed. In the following we provide a summary of the salient experimental finding: (1) The intensities of peaks in the mass spectra of $M_n(Bz)_m^+$ complexes exhibit three different characteristic patterns as one moves along the 3d metal series. For $M_n(Bz)_m^+$ complexes, (M = Sc, Ti, V), prominent peaks occur at $(n,m) = (n,n+1)$ with peak intensities decreasing rapidly with increasing n. The intensities of these structures remained unchanged even after increasing the partial pressure of benzene vapor. With increasing pressure of metal vapor, peaks occus at $(n+1,n)$ but these clusters are reactive. For $Cr_nBz_m^+$ and $Mn_nBz_m^+$, only one major peak

[†] Michigan Technological University.
[‡] Virginia Commonwealth University.
[§] Universidad de Oviedo.

(1) *Comprehensive Organometallic Chemistry*; Wilkinson, G., Stone, F. G. A., Abel, E. W., Eds.; Pergamon: New York, 1982.
(2) Braga, D.; Dyson, P. J.; Grepioni, F.; Johnson, F. G. *Chem. Rev.* **1994**, *94*, 1585.
(3) Ma, J. C.; Dougherty, D. A. *Chem. Rev.* **1997**, *97*, 1303.
(4) Dougherty, D. A. *Science* **1996**, *271*, 163.
(5) Caldwell, J. W.; Kollman, P. A. *J. Am. Chem. Soc.* **1995**, *117*, 4177.
(6) Jacobson, D. B.; Freiser, B. S. *J. Am. Chem. Soc.* **1984**, *106*, 3900.
(7) Jacobson, D. B.; Freiser, B. S. *J. Am. Chem. Soc.* **1984**, *106*, 4623.
(8) Rufus, D.; Ranatunga, A.; Freiser, B. S. *Chem. Phys. Lett.* **1995**, *233*, 319.
(9) Afzaal, S.; Freiser, B. S. *Chem. Phys. Lett.* **1994**, *218*, 254.
(10) Willey, K. F.; Cheng, P. Y.; Bishop, M. B.; Duncan, M. A. *J. Am. Chem. Soc.* **1991**, *113*, 4721.
(11) Willey, K. F.; Yeh, C. S.; Robbins, D. L.; Duncan, M. A. *J. Phys. Chem.* **1992**, *96*, 9106.
(12) Chen, Y. M.; Armentrout, P. B. *Chem. Phys. Lett.* **1993**, *210*, 123.
(13) Meyer, F.; Khan, F. A.; Armentrout, P. B. *J. Am. Chem. Soc.* **1995**, *117*, 9740.
(14) Dunbar, R. C.; Klippenstein, S. J.; Hrusak, J.; Stöckigt, D.; Schwartz, H. *J. Am. Chem. Soc.* **1996**, *118*, 5277.
(15) Ho, Y. P.; Yang, Y.; Klippenstein, S. J.; Dunbar, R. C. *J. Phys. Chem.* **1997**, *101*, 3338.
(16) Hoshino, K.; Kurikawa, T.; Takeda, H.; Nakajima, A.; Kaya, K. *J. Phys. Chem.* **1995**, *99*, 3053.
(17) Judai, K.; Hirano, M.; Kawamata, H.; Yabushita, S.; Nakajima, A.; Kaya, K. *Chem. Phys. Lett.* **1997**, *270*, 23.
(18) Reddic, J. E.; Robinson, J. C.; Duncan, M. A. *Chem. Phys. Lett.* **1997**, *279*, 203.
(19) Nakajima, A.; Nagano, S.; Takeda, H.; Kurikawa, T.; Kaya, K. *J. Chem. Phys.* **1997**, *107*, 6491.
(20) Weis, P.; Kemper, P. R.; Bowers, M. T. *J. Phys. Chem. A* **1997**, *101*, 8207.
(21) Lin, C. Y.; Chen, Q.; Chen, H.; Freiser, B. S. *J. Phys. Chem. A* **1997**, *101*, 6023.
(22) Kurikawa, T.; Takeda, H.; Hirano, M.; Judai, K.; Arita, T.; Nagao, S.; Nakajima, A.; Kaya, K. *Organometallics* **1999**, *18*, 8, 1430.

10.1021/ja0035452 CCC: $20.00
Published on Web 03/28/2001

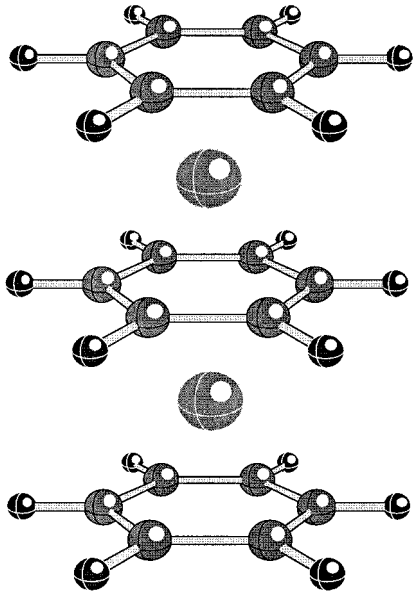

Figure 1. Sandwich structure of metal−benzene complexes where metal atoms are intercalated between benzene planes.

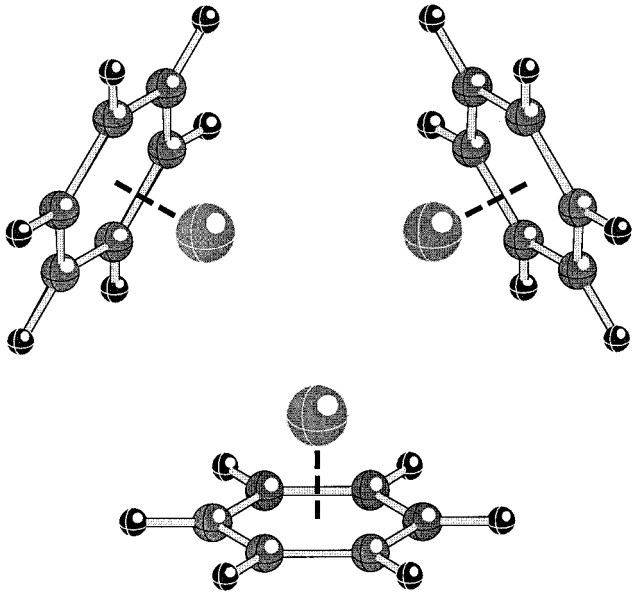

Figure 2. "Rice-ball" structure of metal−benzene complexes where benzene molecules coat the metal atoms.

occurs at $(n,m) = (1,2)$. The above pattern indicates that the likely structure of M_nBz_m (M = Sc to Cr) with $m = n + 1$ is that of a sandwich (see Figure 1) where the metal atoms are intercalated between the benzene molecules. This hypothesis is further supported by the fact that these clusters are not reactive toward reagent molecules such as CO and NH_3 since metal atoms sandwiched between benzene molecules are not exposed for further reaction. Mobility experiments[20] also support this conclusion. $Co_nBz_m^+$ complexes, on the other hand, exhibit mass peaks at $(n,m) = (1,2)$, (2,3), (3,3), (4,4), (5,4), (6,4), ... while the peaks in $Ni_n\ Bz_m^+$ occur at $(n,m) = (1,2)$, (2,2), (3,2), (2,3), (3,3), (4,3), (5,3), (6,3), (6,4), ... Note that in these complexes the metal contents can exceed that of benzene and the maximum number of benzene molecules seldom exceed $m = 4$. More importantly, the peaks beyond $(n,m) = (1,2)$ in these complexes have similar intensities. By further observing that $Co_n(Bz)_4$ and $Ni_n(Bz)_4$ are unreactive toward NH_3, Kaya and co-workers[22] concluded that Co_nBz_m and Ni_nBz_m may have an entirely different structure than those of early transition metal−benzene complexes. For these complexes they have proposed an alternate structure termed "rice-ball" (see Figure 2). Recent mobility experiments[23] also support this assignment. $Fe_nBz_m^+$ complexes do exhibit a pattern of peaks that bear some resemblance to those of Co− and Ni−benzene complexes, although the intensities beyond $(n,m) = (2,3)$ are markedly reduced. (2) The ionization potentials of MBz complexes show the same variation as those in the metal atoms across the 3d series, namely, they are nearly constant from Sc to Cr, rise sharply from Cr to Mn, and again remain nearly unchanged from Fe to Ni. In addition, they are uniformly lowered from their respective values in metal atoms by more than 1 eV. In $M(Bz)_2$ complex, the ionization potential increases from M = Sc to V, shows a minimum at Mn, and then rises steadily from Fe to Ni. (3) In multidecker complexes of $M_n(Bz)_{n+1}$, the ionization potentials decrease with increasing n for M = Sc, Ti, V, but exhibit different behavior in $Co_n(Bz)_m$ and $Ni_n(Bz)_m$ clusters. (4) The dissociation energies[13] of neutral (positively charged) MBz (M = Sc to Ni) reach a minimum at Cr (Mn) and rise as one moves away across the 3d series in either direction. (5) Although there have been no experiments on the total electron spin of the gas-phase metal−benzene complexes, electron paramagnetic resonance (EPR) and electron spin resonance (ESR) measurements[24−26] of metal−benzene complexes in matrices have revealed low-spin ground states. In contrast, free transition metal atoms tend to have high spins.

Theoretical efforts in understanding the geometric structure, dissociation energies, and electronic structure of transition metal atom−benzene complexes have been rather limited. Some of the early theoretical works on neutral and cationic V−benzene complex were performed by Mattar and Hamilton[27] using local spin-density approximation to the density functional theory. Bauschlicher and co-workers[28] were the first to carry out systematic calculations of the cationic $M-Bz^+$ (M = Sc to Cu) complexes using modified coupled pair functional (MCPF) method. They obtained the equilibrium geometries and dissociation energies of these complexes—in good agreement with experiment. A comprehensive analysis of the equilibrium geometries, ionization potentials, electron affinities, electron spin multiplicities, and dissociation energies of MBz complexes using density functional theory and generalized gradient approximation (DFT-GGA) was recently carried out by the present authors.[29] The only theoretical work that we are aware of on multidecker metal−benzene complexes was performed by Bowers and co-workers[20] on $V_n(Bz)_m^+$ clusters using the DFT-GGA level of theory.

In this paper we provide the first systematic theoretical account of the $M(Bz)_2$ complexes (M = Sc to Ni) by carrying out structure optimization of neutral, cationic, and anionic species. We have calculated the metal−benzene distance, dissociation energy, ionization potential, electron affinity (E.A.), and electron spin multiplicity of each of these complexes. In addition, we have studied multidecker complexes involving $V_2(Bz)_3$ and $Fe_2(Bz)_3$. The calculations are performed at the DFT-

(23) Bowers, M. (private communication).

(24) Cloke, F. G. N.; Dix, A. N.; Green, J. C.; Perutz, R. N.; Seddon, E. A. *Organometallics* **1983**, *2*, 1150.
(25) Andrews, M. P.; Mattar, S. M.; Ozin, G. A. *J. Phys. Chem.* **1986**, *90*, 744.
(26) Andrews, M. P.; Mattar, S. M.; Ozin, G. A. *J. Phys. Chem.* **1986**, *90*, 1037.
(27) Mattar, S. M; Sammynaiken, R. *J. Chem. Phys.* **1997**, *106*, 1080.
(28) Mattar, S. M.; Hamilton, W. *J. Phys. Chem.* **1989**, *93*, 2997.
(29) Bauschlicher, C. W.; Partridge, H.; Langhoff, S. R. *J. Phys. Chem.* **1992**, *96*, 3273.

GGA level of theory. The results not only provide an explanation of all existing experimental data in these systems, but also predict new results such as electron affinities and magnetic properties that could be verified experimentally.

In section II we outline briefly our theoretical procedure. Results on MBz and $M(Bz)_2$ complexes are discussed in section III. The properties of multidecker complexes involving $V_2(Bz)_3$ and $Fe_2(Bz)_3$ are discussed in Section IV. A summary of our conclusions is contained in Section V.

II. Theoretical Procedure

The calculations were performed using the linear combination of atomic orbital-molecular orbital (LCAO-MO) theory. The atomic orbitals were represented by a double numerical basis with polarization functions (DNP). The exchange-correlation potentials were approximated by using the generalized gradient approximation (GGA) to the density functional theory (DFT). We have used, in particular, the Becke form for exchange and Perdew−Wang form for correlation which is commonly referred to as BPW91.[30] The electron spin multiplicity was determined using the *aufbau* principle where one successively fills the molecular energy levels in keeping with the Pauli exclusion principle. All calculations were carried out using the DMOL code.[31]

In our earlier work[29] we had checked the accuracy of this procedure by carrying out separate calculations for benzene and FeBz complex using three different Gaussian atomic bases (6-311G**, 3-21G**, and LanL2DZ) and the Gaussian 94 code,[32] but the same approximation for the exchange-correlation functional. The results using the numerical bases agreed very well with those using the various Gaussian bases. In addition, the spin multiplicities obtained using the *aufbau* principle were also in agreement with those obtained by explicit energy minimization of various spin multiplet structures.

We should, however, caution the reader about one of the difficulties associated with the density functional theory in treating the spin-multiplet structures of transition metal systems. Due to their open d-shell structure, transition metal systems have many spin-multiplet structures within a narrow energy range. Although the density functional theory can yield the lowest-energy state in each particular symmetry (spatial and spin) channel, the calculations will tend to favor systems with highest spin multiplicities. This spin contamination problem has been discussed extensively [33−36] in the literature, and generally, Kohn−Sham orbitals provide wave functions with a much smaller spin contamination than the unrestricted Hartree−Fock methods do. Higher-level theories where electronic wave functions are treated as multistates determinants would be necessary to validate the accuracy of the density functional methods. As is well-known, such methods (e.g., MCSCF, CASSCF, ...) are computer intensive and cannot treat systems involving multiple transition metal atoms and benzene complexes. Recently Gutsev et al. have systematically studied[37] the electronic and geometrical structure of the ground and excited states of 3d transition metal monoxides using density functional theory and various forms for the generalized gradient approximation for exchange correlation potential. They have compared their results with those obtained by Bauschlicher and Maitre[38] using the infinite order coupled cluster method with all singles and doubles and noniterative inclusion of triple excitations (CCSD(T)) method and experiment. The agreement including ground-state electronic configuration is very good, and the BPW91 form for the DFT-GGA was found to be more preferable over other forms. In addition, as we have shown earlier,[29] the density functional results including spin multiplicities of M^+−benzene (M = 3d atom) agree very well with those of Bauschlicher et al.[28] who used MCPF method. To establish further confidence on our DFT-GGA procedure, we have calculated the equilibrium geometry, spin multiplicity, and dissociation energy of of $Cu(Bz)^+$ complex using the same numerical procedure as used for all 3d metal−benzene complexes in this work. Note that Bauschlicher et al.[28] had studied this system extensively by using CCSD and CCSD(T) methods in addition to the MCPF method as well as various levels of basis sets. All of their calculations yielded a singlet ground state with dissociation energies ranging from 2.12 to 2.32 eV. Our calculated spin multiplicity and dissociation energy for $CuBz^+$ are 1 and 2.55 eV, respectively. Our calculated distance of the Cu atom from the plane of the benzene ring, the C−C distance, and C−H distance are 1.78, 1.42, and 1.08 Å respectively. These agree very well with the MCPF results of Bauschlicher et al.[28] which are 1.85, 1.42, and 1.07 Å, respectively. We will show later in this paper that our calculated spin multiplicities of $Ti(Bz)_2$, $Ti(Bz)_2^+$, $V(Bz)_2$, $V(Bz)_2^+$, and $Cr(Bz)_2^+$ are identical to those measured in ESR experiments.[24]

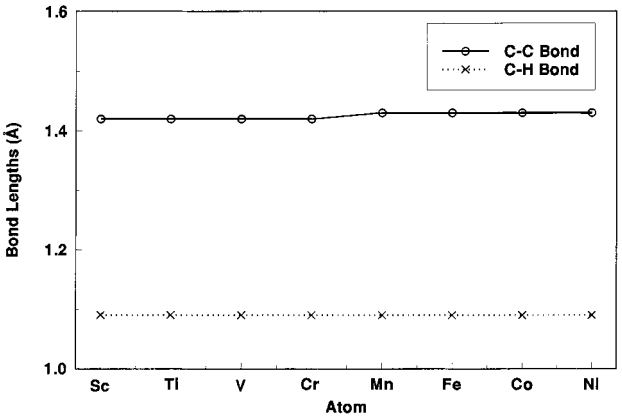

Figure 3. C−C and C−H bond distances in optimized structure of MBz complexes for M = Sc to Ni.

The geometry optimization in our previous MBz work[29] was carried out without any symmetry constraint. However, upon global optimization, all of the structures were found to possess C_{6v} symmetry in which the metal atom sits on top of the benzene plane along a line passing through its center of mass. The optimized C−C and C−H distances in neutral MBz complexes are shown in Figure 3 for M = Sc to Ni. Note that there is virtually no change in the C−C and C−H bond distances across the 3d series. We expect that in larger complexes of $M_n(Bz)_m$, the C−C and C−H bond distances would also remain the same as those in pure benzene. In our geometry optimization of the $M_n(Bz)_m$ multidecker complexes, we have, therefore, used the D_{6h} symmetry and allowed only the metal atom distance from each of the benzene plane to vary. We will show that while such a symmetry constraint may be appropriate for M = Sc to Fe, the study of Co_nBz_m and Ni_nBz_m complexes may require extra care. In the following we present the results of our calculations.

III. Properties of MBz and $M(Bz)_2$ [M = Sc−Ni]

In this section we discuss the geometries, electronic structure, ionization potentials, dissociation energies, electron affinities,

(30) Pandey, R.; Rao, B. K.; Jena, P.; Newsam, J. M. *Chem. Phys. Lett.* **2000**, *321*, 142.
(31) Becke, A. D.; *Phys. Rev.* A **1988**, *38*, 3098; Perdew, J. P.; Chevary, J. A.; Vosko, S. H.; Jackson, K. A.; Pederson, M. R.; Singh, D. J.; Fiolhais, C. *Phys. Rev.* B **1992**, *46*, 6671; Perdew, J. P.; Chevary, J. A.; Vosko, S. H.; Jackson, K. A.; Pederson, M. R.; Singh, D. J.; Fiolhais, C. *Phys. Rev.* **1993**, *48*, 4978.
(32) *DMOL Code*; Biosym Technologies, Inc.: San Diego, CA, 1995.
(33) Frisch, M. J.; Trucks, G. W.; Schlegel, H. B.; Gill, P. M. W.; Johnson, B. G.; Robb, M. A.; Cheeseman, J. R.; Keith, T.; Petersson, G. A.; Montgomery, J. A.; Raghavachari, K.; Al-Laham, M. A.; Zakrzewski, V. G.; Ortiz, J. V.; Foresman, J. B.; Cioslowski, J.; Stefanov, B. B.; Nanayakkara, A.; Challacombe, M.; Peng, C. Y.; Ayala, P. Y.; Chen, W.; Wong, M. W.; Andres, J. L.; Replogle, E. S.; Gomperts, R.; Martin, R. L.; Fox, D. J.; Binkley, J. S.; Defrees, D. J.; Baker, J.; Stewart, J. P.; Head-Gordon, M.; Gonzalez, C.; Pople, J. A. *Gaussian 94*, revision B.1; Gaussian, Inc.: Pittsburgh, PA, 1995.
(34) Wang, J.; Becke, A. D.; Smith, V. H. J., Jr. *Chem. Phys.* **1985**, *102*, 3477.
(35) Cramer, C. J.; Dulles, F. J.; Giesev, D. J.; Almlöf, J. *Chem. Phys. Lett.* **1995**, *245*, 165.
(36) Görling, A.; Trickey, S. B.; Gisdakis, P.; Rösch, N. *Top. Organomet. Chem.* Hoffman, P., Brown, J. M., Eds.; Springer: Heidelberg, 1999: Vol. 4, pp 109−165.
(37) Wittbrodt, J. M.; Schlegel, H. B. *J. Chem. Phys.* **1996**, *105*, 6574.
(38) Gutsev, G. L.; Rao, B. K.; Jena, P. *Phys. Chem. A* **2000**, *104*, 5374.

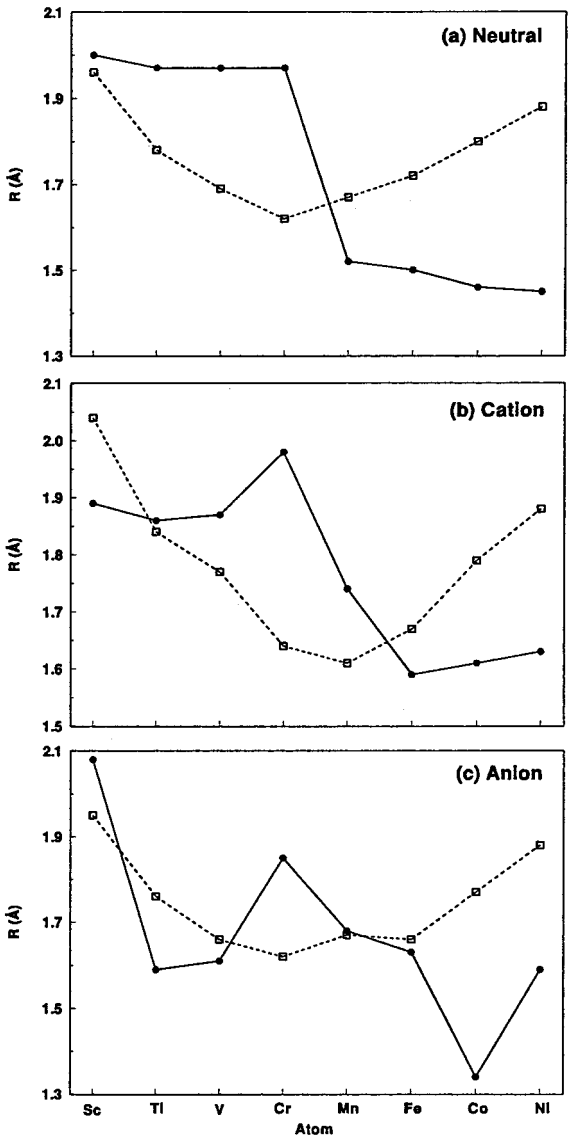

Figure 4. Distances of metal atoms from the center of the benzene ring in neutral, cationic, and anionic metal−benzene complexes. The solid circles correspond to MBz complexes, while the open squares correspond to $M(Bz)_2$ complexes.

and magnetic properties of $M(Bz)_2$ complexes and compare the results with those of MBz and the free metal atoms across the 3d series.

A. Geometries. As pointed out earlier, the geometries of the MBz complexes, after a global search, were found[29] to have a C_{6v} symmetry with the metal atom sitting on top of the center of the benzene ring at a distance *d*, along the center of mass axis. These distances are plotted in Figure 4a−c for the optimized neutral, cationic, and anionic MBz complexes (solid circles) and compared with those belonging to the $M(Bz)_2$ series (open squares). We want to remind the reader that the structures of $M(Bz)_2$ were optimized with the D_{6h} symmetry constraint with the metal atom sandwiched between two benzene planes (see Figure 1). While such structures are valid for M = Sc to Cr and possibly for Fe, the structures of $Co(Bz)_2$ and $Ni(Bz)_2$ as pointed out by Kaya and co-workers may be somewhat different. Our results suggest that this, indeed, may be the case as the agreement between theory and experiment is good for M = Sc to Fe but is poor for Co and Ni.

We note from Figure 4a that in neutral MBz complexes, 3d metal atoms from Sc to Cr are at a distance of about 2Å from the benzene plane, while those from Mn to Ni lie at a distance of about 1.5Å. This stepwise variation of the benzene−metal atom distance across the 3d series is also somewhat present (see Figure 4b) in the cationic MBz^+ complexes. No such clear pattern emerges in the anionic MBz^- complexes (see Figure 4c). The corresponding bond distances for the $M(Bz)_2$ are compared with the above in Figure 4. Note not only that these distances are qualitatively different from those in MBz complexes but also that their variations across the 3d series are similar for neutral, cationic, and anionic configurations; namely, they decrease from Sc to Cr and then rise from Mn to Ni. Furthermore, the metal−benzene distances in $M(Bz)_2$ are smaller than those of MBz for M = Sc to Cr and larger for M = Fe, Co, Ni.

Table 1. Valence Configurations of M−(Bz) Complexes Where M Is a Transition Metal Atom

metal	valence configuration	multiplicity (2S+1)
Sc	$(3de_2)^2$, $(4sa_1)^1$	4
Ti	$(3de_2)^2$, $(4sa_1)^1$, $(3da_1)^1$	5
V	$(3de_2)^2$, $(4sa_1)^1$, $(3de_1)^2$	6
Cr	$(3de_2)^2$, $(4sa_1)^1$, $(3de_1)^2$, $(3da_1)^1$	7
Mn	$(3de_2)$,^{4} $(4sa_1)^1$, $(3de_1)^2$	4
Fe	$(3de_2)$,^{4} $(4sa_1)^2$, $(3de_1)^2$	3
Co	$(3de_2)$,^{4} $(4sa_1)^2$, $(3de_1)^3$	2
Ni	$(3de_2)$,^{4} $(4sa_1)^2$, $(3de_1)^4$	1

B. Electronic Structure. The electronic structure of MBz and $M(Bz)_2$ complexes can be studied by analyzing the nature of the highest occupied molecular orbitals (HOMO). Assuming that 3d and 4s orbitals of the transition metal interact with six ligand orbitals ($2p_z$ orbitals in benzene) to form the valence orbitals of these complexes, the strength of their interaction would determine the electronic properties of these complexes. In the present study, a stronger interaction is expected for $M-(Bz)_2$ complexes, which leads to a larger splitting of the orbitals, thereby facilitating the pairing of electrons. On the other hand, a weaker interaction is expected for M−(Bz) complexes, yielding largely unpaired configurations. The molecular orbital energy levels of M−(Bz) and $M-(Bz)_2$ complexes appear to conform to the high-spin (weak-field) and low-spin (strong-field) orbital filling schemes, respectively.

The valence configuration of the (isolated) transition metal atoms is $3d^n\ 4s^2$ (except for Cr which is $3d^5\ 4s^1$), whereas that of (isolated) benzene is $a_{2u}^2\ e_{1g}^4$ in the D_{6h} symmetry. In the M−(Bz) complex with C_{6v} symmetry, the ligand orbitals will not generally be placed between the metal orbitals, and the expected order of valence orbitals will be a_1, e_1 (from occupied a_{2u} and e_{1g} orbitals of benzene), 4s/3d (partially filled, from transition metal atom), and e_2, b_2 (from unoccupied e_{2u} and b_{2g} orbitals of benzene). Since the 3d orbitals split into $3da_1$ (d_{z^2}), $3de_1$ (d_{xz} and d_{yz}), and $3de_2$ ($d_{x^2-y^2}$ and d_{xy}) in a C_{6v} field, the metal−ligand orbital interaction can be classified in terms of the interactions between a_1(Bz) $4sa_1$(M) $3da_1$(M), e_1(Bz) $3de_1$(M) and $3de_2$(M) e_2(Bz) orbitals.

The calculated valence configurations obtained in the present study for M−(Bz) complexes are given in Table 1. The corresponding molecular energy levels are given in Figure 5. According to them, orbital splitting is not large enough for paired-electron configurations to be preferred, yielding a dominance of the maximum spin multiplicity configurations. Both $4sa_1$ and $3de_2$ orbitals tend to be filled, whereas the $3da_1$ orbital gradually moves to higher energies in going from Sc to Ni. A closer examination of the $3da_1$ orbital reveals it to be an antibonding orbital. The metal−ligand distance will be larger when an antibonding orbital is occupied than when a bonding

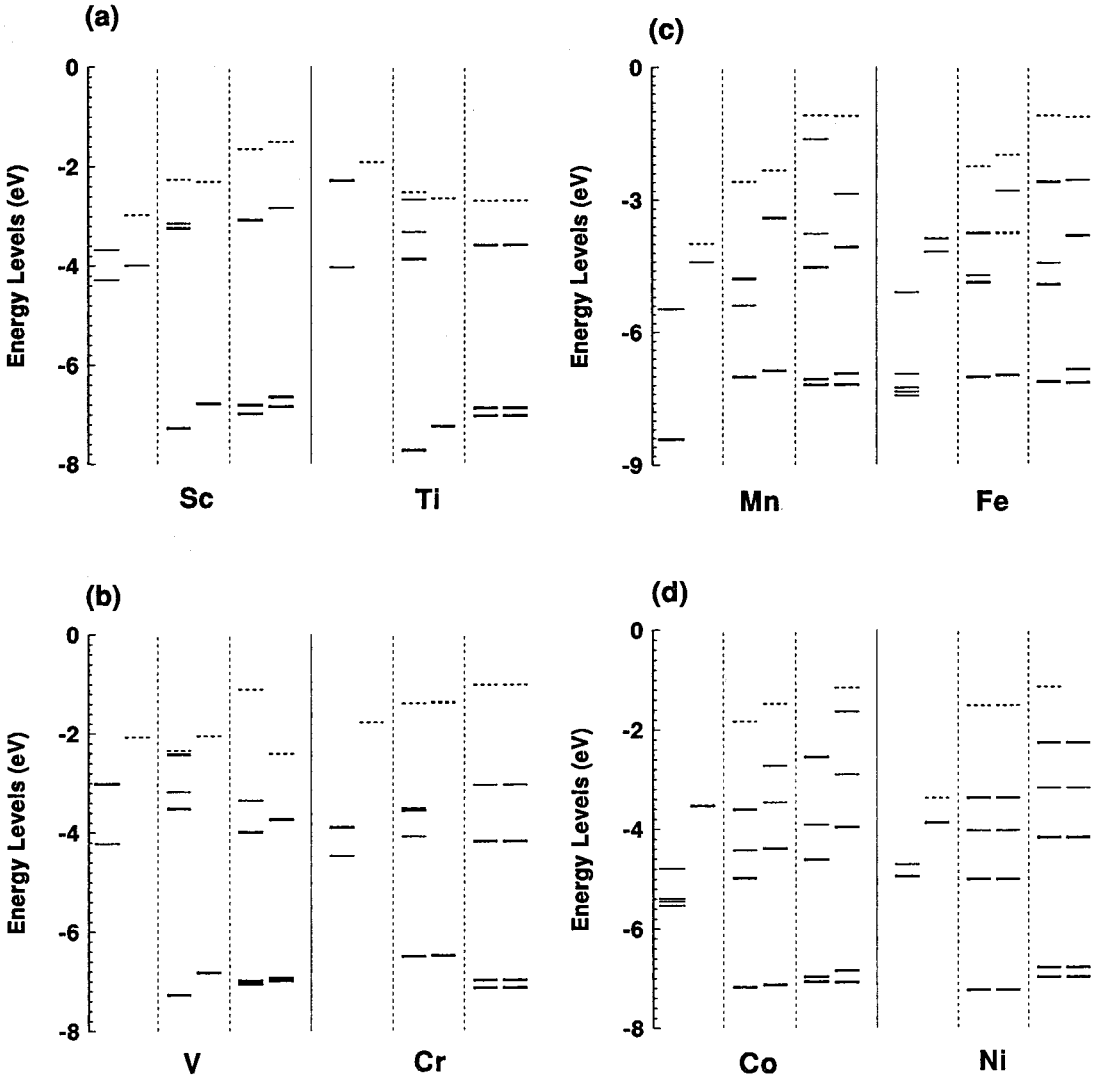

Figure 5. Molecular orbital energy levels of M, MBz, and $M(Bz)_2$ complexes.

Table 2. Valence Configurations of $M-(Bz)_2$ Complexes Where M Is a Transition Metal Atom

metal	valence configuration	multiplicity (2S+1)
Sc	$(3de_{2g})^3$	2
Ti	$(3de_{2g})^4$	1
V	$(3de_{2g})^4$, $(4sa_{1g})^1$	2
Cr	$(3de_{2g})^4$, $(4sa_{1g})^2$	1
Mn	$(3de_{2g})^4$, $(4sa_{1g})^2$, $(3de_{1g})^1$	2
Fe	$(3de_{2g})^4$, $(4sa_{1g})^2$, $(3de_{1g})^2$	3
Co	$(3de_{2g})^4$, $(4sa_{1g})^2$, $(3de_{1g})^3$	2
Ni	$(3de_{2g})^4$, $(4sa_{1g})^2$, $(3de_{1g})^4$	1

orbital is occupied. For example, the calculated metal−ligand distance decreases from 1.97 Å (Cr−Bz) to 1.52 Å (Mn−Bz) when an electron prefers to occupy a bonding orbital ($3de_2$) over an antibonding orbital ($3da_1$).

For $M-(Bz)_2$ complexes, the valence configurations in the D_{6h} symmtery are listed in Table 2. We find that electrons prefer to be paired in bonding orbitals (i.e., strong-field case) in going from Sc to Ni. Orbital interactions are analogous to those in M−Bz complexes, only changing the symmetry labels to a_{1g}, e_{1g}, and e_{2g}, respectively. In this case, $3da_{1g}$ (d_{z^2}) is an antibonding orbital and remains unoccupied. Moreover, the $3de_{1g}$ (d_{xz} and d_{yz}) orbitals appear to have an antibonding character due to their interaction with the two occupied benzene e_{1g} orbitals. Having electrons occupying the $3de_{1g}$ orbitals increases the metal−ligand distance for Mn to Ni, as shown in Figure 4.

C. Ionization Potential. The ionization potential is defined as the difference in the total energies of the neutral and positively charged cluster. Since clusters generally relax following their ionization, the difference in the total energies of the ground states of the neutral and cationic cluster is referred to as the adiabatic ionization potential (A.I.P.). The total energy difference between the ground state of the neutral and the cation having the geometry of the neutral ground state, on the other hand, is referred to as the vertical ionization potential (V.I.P.).

In Figure 6b,c we plot the vertical ionization potentials of MBz and $M(Bz)_2$ complexes and compare them with those of the free metal atom, M (Figure 6a). The experimental values, which correspond to vertical ionization, are given as open squares. The adiabatic ionization potentials can be evaluated from the total energies of the neutral and cation ground states. In almost all cases the adiabatic ionization potentials are within 0.1 eV of the vertical values, indicating little geometrical changes following ionization.

Note that the ionization potentials of Sc, Ti, V, and Cr atoms are nearly the same (6.7 ± 0.1 eV) while those of Fe, Co, and Ni are about 1 eV higher but also nearly constant (see Figure 6a). The ionization potentials of MBz complexes (Figure 6b) are not only uniformly lowered from their values of the free metal atoms by about 1 eV but also show the characteristic step at Mn.

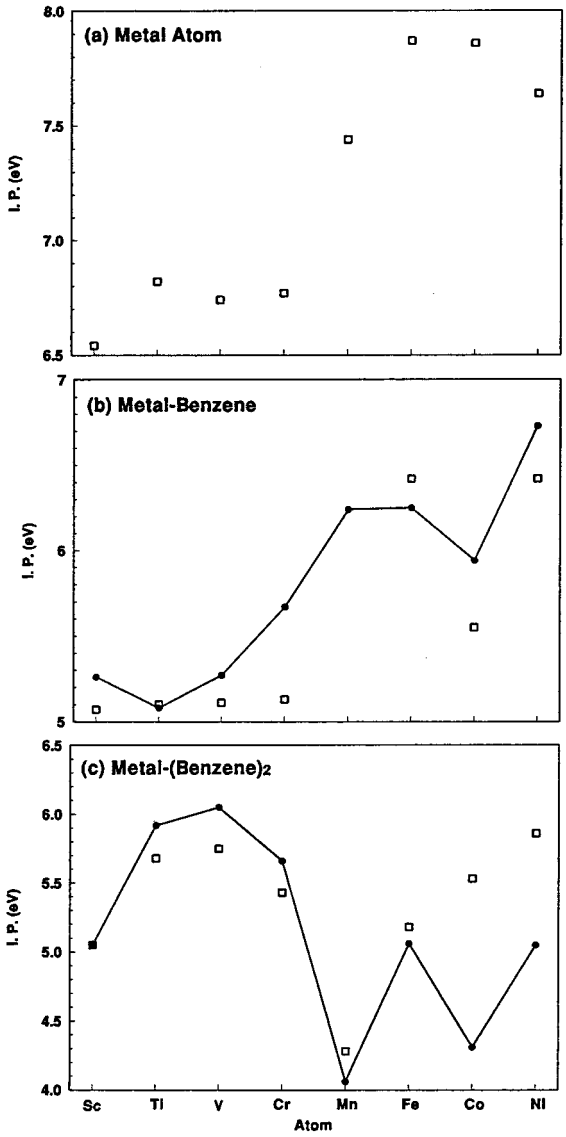

Figure 6. Vertical ionization potentials of (a) metal atom, (b) MBz, and (c) $M(Bz)_2$. The solid circles are calculated values, where the open squares correspond to experiment.

The ionization potentials of $M(Bz)_2$ complexes (see Figure 6c), on the other hand, show a very different behavior across the 3d series. They increase from Sc to Ti, by almost 1 eV and then decrease from V- to Mn-containing complexes. The variations in the ionization potentials of M, MBz, and $M(Bz)_2$ complexes across the 3d series can be understood by comparing their HOMO energy levels in Figure 5 and by examining their electronic state. Note that the interaction of the benzene Π electrons with the 3d electrons of the transition metals gives rise to charge transfer and hence to a shift in the HOMO levels. As the HOMO level shifts to higher energy, the ionization potential is expected to decrease. This is, indeed, the case between free 3d metal atoms and those supported on a single benzene molecule. Note from Figure 5 that with the only exception of TiBz, the HOMO levels of all MBz complexes are shifted upward in energy, causing the ionization potentials to drop. In $M(Bz)_2$ complexes, the HOMO levels for M = Sc, Cr, Mn, Fe, Co, and Ni are shifted upward in comparison to the corresponding MBz complexes and thus should cause their ionization potentials to be lowered. This is, indeed, the case for Mn, Fe, Co, and Ni as seen in Figure 6. For $Sc(Bz)_2$ and $Cr(Bz)_2$, the ionization potentials are nearly equal to those of ScBz and CrBz, respectively. Similarly, the HOMO levels of $Ti(Bz)_2$ and $V(Bz)_2$ in Figure 5 are lowered in comparison to those of TiBz and VB_z respectively. Correspondingly, the ionization potentials of $Ti(Bz)_2$ and $V(Bz)_2$ should be higher than that of TiBz and VBz. Results in Figure 6 confirm this. Not only do the theoretical values reproduce the experimental trend from Sc to Fe in $M(Bz)_2$ complexes, but the magnitudes are also in good agreement. However, the agreement between theory and experiment is rather poor for $Co(Bz)_2$ and $Ni(Bz)_2$. While the experimental ionization potentials increase from $Fe(Bz)_2$ to $Ni(Bz)_2$, the theoretical values oscillate. Since all of the 3d elements are treated at the same level of theory, the poor agreement for Co− and Ni−benzene complexes indicate the possibility that the structure of $Co(Bz)_2$ and $Ni(Bz)_2$ may not be the same as that in Figure 1. We will comment on this possibility later.

D. Dissociation Energies. The relative stability of the MBz complexes as M varies from Sc to Ni can be studied by evaluating the energy needed to dissociate a MBz complex into M and Bz fragments. We define this dissociation energy, D_e as

$$D_e = -\{E[\mathrm{MBz}] - E[\mathrm{Bz}] - E[\mathrm{M}]\}$$

where E[MBz], E[Bz], and E[M] are the total energies of the MBz complex, benzene molecule, and metal atom, respectively. We have neglected contributions from zero-point energies in all our calculations. We term the dissociation energy of the neutral MBz complex as D_e^o and that of the positively charged MBz^+ complex as D_e^+. D_e^+ is evaluated by subtracting from the total energy of MBz^+ the energy of the neutral benzene and cationic metal atom, M^+. The results are plotted in Figure 7b,c. Note that both D_e^o and D_e^+ exhibit similar patterns, namely, they reach a minimum around Cr and Mn, respectively, and increase as one moves along either direction of the 3d series.

This behavior can be understood from the electronic properties of the 3d atoms. Note that all of elements in the 3d series except Cr have $3d^n\ 4s^2$ configuration. As the 3d elements are adsorbed onto benzene, the atomic configuration of these metal atoms changes to $3d^{n+1}\ 4s^1$ configuration due to Pauli repulsion. The $4s^1$ electron, then, has the option to align either parallel or antiparallel with the $3d^{n+1}$ electrons. According to the Hund's rule, the state with highest spin multiplicity would have the lowest energy. Thus, the $4s^1$ electron should prefer to align parallel to the majority spin of $3d^{n+1}$ electrons. However, what is more meaningful in terms of its bonding to benzene is the energy cost for flipping the $4s^1$ spin. The lower this energy, the stronger should be the bonding of the metal atom to benzene. This, indeed, is the case. In Figure 7a we plot the spin-flip energy Δ of the $4s^1$ electron of 3d metal atoms from Sc to Ni. Note that this energy rises from Sc to Cr and then declines toward Ni. This behavior is opposite to the trend of the dissociation energy of the MBz complex (see Figure 7b); namely, the highest spin-flip energy of Cr atom is associated with the weakest bonding of Cr to benzene. Thus, the trend of the dissociation energies of MBz complexes has a magnetic origin. The significant increase in the magnitude of D_e^+ compared to that of D_e^o (by almost 1 eV) is due to the fact that metal cations gain additional binding energy by their ability to polarize the benzene molecule.

The dissociation energy of the neutral $M(Bz)_2$ complex is defined as the energy needed to dissociate the complex into MBz + Bz, namely,

$$D_e^{\,o}[\mathrm{M(Bz)_2}] = -\{E[\mathrm{M(Bz)_2}] - E[\mathrm{MBz}] - E[\mathrm{Bz}]\}$$

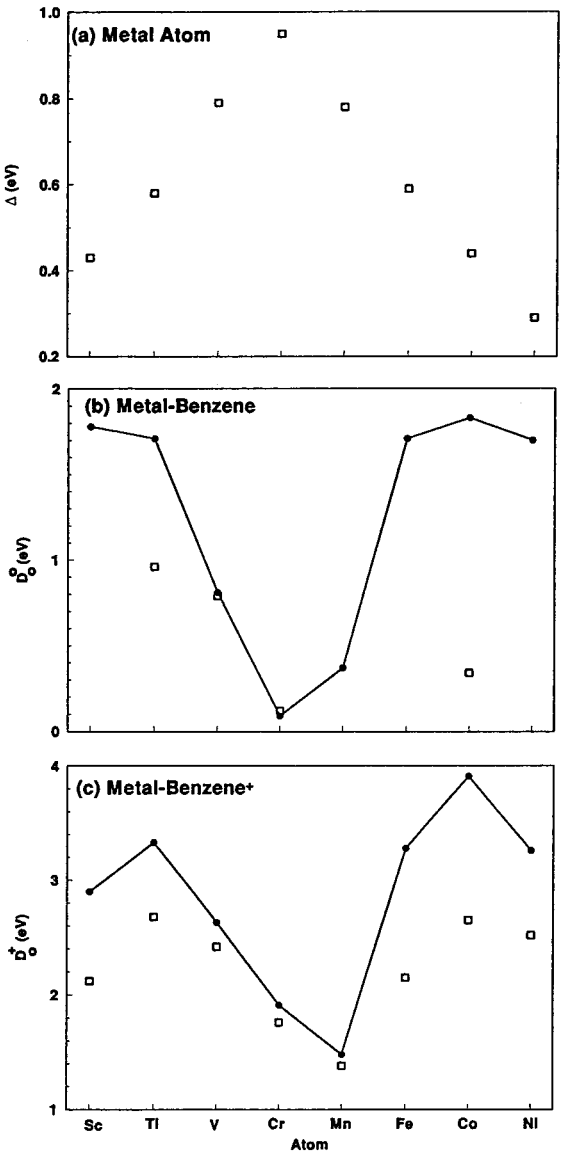

Figure 7. Dissociation energies of (b) neutral and (c) cationic MBz complexes. The solid circles are our theoretical values, while the open squares represent experiment (see ref 22). The spin-flip energies of the $4s^1$ electron of the metal atoms are plotted in (a).

Similarly, the dissociation energy of the cationic $M(Bz)_2^+$ complex into MBz^+ and Bz fragments is defined as,

$$D_e^+[M(Bz)_2^+] = -\{E[M(Bz)_2^+] - E[MBz^+] - E[Bz]\}$$

Experimentally D_e^+ is determined from collision-induced dissociation. Experimental values of D_e^o for the neutral $M(Bz)_2$ complex can be inferred from the equation,

$$D_e^o[M(Bz)_2] = D_e^+[M(Bz)_2^+] + \text{I.P.}[M(Bz)_2] - \text{I.P.}[MBz]$$

where I.P. represents experimental ionization potentials of the corresponding complexes. In Table 3 we compare the values of the dissociation energies with experiment for neutral and cationic $M(Bz)_2$ complexes.

Note that for elements from Sc to Mn, the addition of an extra benzene molecule significantly increases the binding energy of the $M(Bz)_2$ complex. Experimental values of the dissociation energies of neutral $M(Bz)_2$ complexes could not be evaluated for Sc, Mn, Fe, and Ni systems as the ionization potentials of $M(Bz)_2$ complexes for M = Mn, Fe, and Ni are either unavailable or their values are not known precisely. Similarly, no experimental information on the dissociation energy of cationic $Sc(Bz)_2^+$ is available. The agreement between the calculated and experimental values of $D_e^o[M(Bz)_2]$ for M = Ti, V, and Cr is very good. However, the agreement for $Co(Bz)_2$ is poor and we suspect similar fate will befall $Ni(Bz)_2$. This disagreement suggests again that the structure of these two complexes may not have the D_{6h} symmetry, and the two benzene planes may be tilted. We are currently carrying out full geometry optimization without any symmetry constraint for $Co(Bz)_2$ and $Ni(Bz)_2$ systems. The results will be published later.[39] We should also point out that the agreement between theory and experiment of the dissociation energies is, in general, inferior to that of the ionization potential. This arises due to the inaccuracies in the total energy of the atoms and their positive ions. This inaccuracy could be significantly reduced by using a more extended basis. Our objective in this work, however, has been to understand the underlying variation in physics and chemistry of transition metal elements interacting with benzene. A more detailed calculation of the Ni−benzene complexes involving multiple Ni atoms and benzene molecules is currently under way. The results will be published in due course.

Table 3. Dissociation Energy (eV) of $M(Bz)_2$ into $MBz+$ Bz for Neutral and Cationic Clusters as Compared to Those of MBz and $M(Bz)_2^+$

	D_e0[MBz]		D_e0[$M(Bz_2)$]		D_e^+[MBz^+]		D_e^+[$M(Bz_2)^+$]	
M	theo.	expt.	theo.	expt.	theo.	expt.	theo.	expt.
Sc	1.78		2.04		2.90	2.12	2.23	
Ti	1.71	0.96	3.32	3.20	3.33	2.68	2.49	2.62
V	0.81	0.79	3.57	3.19	2.63	2.42	2.88	2.55
Cr	0.09	0.12	2.78	2.70	1.91	1.76	2.42	2.40
Mn	0.37		1.18		1.48	1.38	3.19	2.10
Fe	1.71	>0.7	1.09		3.28	2.15	2.26	1.94
Co	1.83	0.34	0.42	1.71	3.91	2.65	1.97	1.73
Ni	1.70	0.87−1.30	0.02		3.26	2.52	1.46	1.52

Of the $M(Bz)_2$ complexes, the dissociation energy of $Cr(Bz)_2$ is the most spectacular: It is nearly 30 times larger than that of the CrBz complex. This remarkable stability of $Cr(Bz)_2$, as pointed out by Kurikawa et al.,[22] is the consequence of the 18-electron rule. Cr, having an electronic configuration of d^5s^1, contributes 6-valence electrons while each benzene molecule contributes 6 electrons. The dissociation energies of $M(Bz)_2^+$ complexes into MBz^+ and Bz agree well with experiment not only in the way they vary across the 3d series but also by the degree to which their magnitudes agree, even in the case of $Co(Bz)_2^+$ and $Ni(Bz)_2^+$ complex. The only exception we find here is that for $Mn(Bz)_2^+$. The calculated dissociation energy is larger than experiment by about 1 eV. In addition, the experimental dissociation energy of $Mn(Bz)_2^+$ is less than those of $V(Bz)_2^+$ and $Ti(Bz)_2^+$. This we find to be surprising as $Mn(Bz)_2^+$ is an 18-electron system and according to Kurikawa et al.[22] should be a very stable complex among the cationic 3d metal−$(benzene)_2$ systems.

E. Spin Multiplicities. The preferred spin multiplicities of the MBz complexes are compared to those of the metal atoms in Table 4. Note that the spin multiplicities of the 3d transition metal atoms with the only exception of Cr are determined by the occupation of their 3d electrons. For example, Sc with a $3d^1\,4s^2$ configuration has one spin-unpaired d electron and hence a spin multiplicity of (2s + 1) = 2. The spin multiplicities increase as the spin-up electrons increase until it reaches the $3d^5$ configuration in Cr. Beyond Mn, the electrons fill the spin-

(39) Bauschlicher, C. W., Jr.; Maitre, P. *Theor. Chim. Acta* **1995**, *90*, 189.

Table 4. Spin Multiplicities, (2s+1) of M, MBz, and $M(Bz)_2$ Complexes (Neutral and Charged) for M = Sc to Ni

	M	MBz	MBz^+	MBz^-	$M(Bz)_2$	$M(Bz)_2^+$	$M(Bz)_2^-$
Sc	2	4	3	3	2	3	1
Ti	3	5	4	2	1	2	2
V	4	6	5	3	2	3	1
Cr	7	7	6	6	1	2	2
Mn	6	4	5	5	2	1	3
Fe	5	3	4	4	3	2	2
Co	4	2	3	1	2	3	1
Ni	3	1	2	2	1	2	2

down 3d orbitals, and the cancellation leads to decreasing spin multiplicities. The spin multiplicities of MBz are larger than those in the metal atoms by two from Sc to V and smaller by two from Mn to Ni. The spin multiplicity of CrBz remains unchanged at 7. This behavior was explained[29] to be a consequence of the Pauli exclusion principle that requires the orbital occupation of the 3d atoms to change from $d^n s^2$ to $d^{n+1} s^1$ configuration in going from free atoms to that bonded to benzene. Note that for less than half-filled d shells (Sc, Ti, V) the promotion of an s electron to the spin-up d orbital enhances the spin multiplicity, while for atoms with half-filled or more than half-filled d shells (Mn, Fe, Co, Ni), the promotion of s into spin-down d states reduces the spin multiplicities. The behavior of the spin multiplicities of MBz^+ complexes can be explained in a similar way.

There have been no experiments on the spin multiplicities of metal−benzene complexes in the gas phase. However, ESR measurements[24−26] on matrix-isolated VBz yield its spin multiplicities to be 2. This would appear to contradict the results in Table 2 where the calculated spin multiplicity of VBz is 6. It should be pointed out that in transition metal systems, due to closely lying d states, the energies corresponding to different spin multiplicities lie very close to each other and small perturbations can often change their spin multiplicities. Thus, it is quite possible that the spin multiplicity of a cluster embedded in a matrix may be affected by the matrix and, thus, may differ from their value in the gas phase. For example, Weis et al.[20] have found that VBz^+ cluster with a spin multiplicity of 5 lies only 2.1 kcal/mol higher than the triplet ground-state configuration. This energy difference the authors have determined to be within the uncertainties in their theoretical method. Bauschlicher and co-workers,[28] on the other hand, have found the ground state of VBz^+ to be 5 as is the case in our calculation.

As a second benzene is attached to either neutral or anionic MBz complex, their spin multiplicities are reduced to their minimum possible value, namely a singlet for even-electron system and doublet for odd-electron system. The only exception we see is in $Fe(Bz)_2$ and $Mn(Bz)_2^-$ systems. Instead of being a singlet, they prefer a triplet spin state. This quenching of the spin due to adsorption of a second benzene molecule reflects the high degree of hybridization between metal d and benzene π states. The spin multiplicities of $M(Bz)_2^+$ complexes do not follow the minimum rule of the neutral and anions. Instead, $Sc(Bz)_2^+$, $V(Bz)_2^+$, and $Co(Bz)_2^+$ correspond to triplet configuration. Our calculated spin multiplicity of $V(Bz)_2^+$ is in agreement with that calculated earlier by Bower and co-workers.[20] There have been no experimental results on the spin multiplicities of transition metal atom−$(benzene)_2$ complexes in the gas phase. However, a comparison of experimental results in the gas phase to those in the bulk in some cases have enabled Kaya and co-workers[22] to deduce the electron spin of some of these complexes. Electron spin resonance experiments[24] of $Ti(Bz)_2$, $Ti(Bz)_2^+$, $V(Bz)_2$, $V(Bz)_2^+$, and $Cr(Bz)_2^+$ have yielded

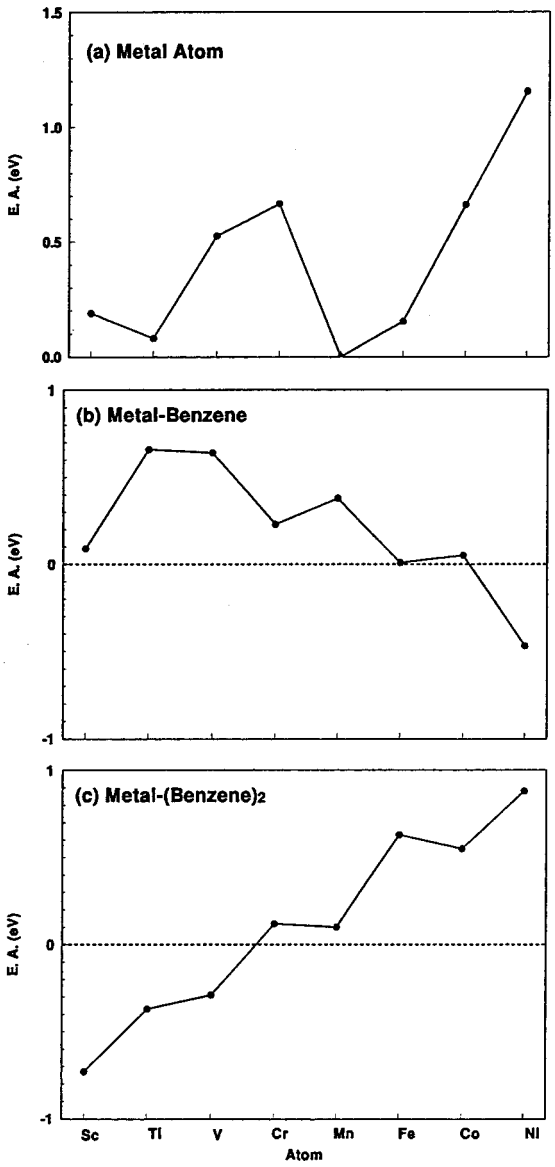

Figure 8. The adiabatic electron affinities of M, MBz, and $M(Bz)_2$ complexes for M = Sc to Ni. The solid circles are our theoretical values. The only experimental value available for VBz system is given as open square.

their spin multiplicities as 1, 2, 2, 3, and 2, respectively. These are in perfect agreement with the results in Table 4.

F. Adiabatic Electron Affinity. The adiabatic electron affinities defined as the energy difference between the ground states of the anion and the neutral are plotted for the MBz complexes in Figure 8b and compared with those of the free atoms in Figure 8a. Note that the variation in the electron affinities in MBz complexes has the opposite trend to that in the metal atoms. Further, the energy gain in attaching an electron to MBz (M = Sc, Fe, and Co) is vanishingly small and negative for NiBz; that is, $NiBz^-$ is unstable toward autodetachment of the extra electron. On the other hand, MBz^- (M = Ti, V, Cr, Mn) complexes have rather sizable electron affinities. There are no systematic experimental studies of the electron affinity of these complexes to our knowledge. Our calculated value of 0.64 eV in VBz agrees very well with the only available experimental data[17] of 0.62 ± 0.07 eV in this series. Similar experiments for the remaining transition metal−benzene complexes will be helpful.

Table 5. Valence Configurations of $M(Bz)_2$ Complexes Corresponding to Neutral ($q = 0$) and Anionic ($q = -1$) Configurations; Electron Affinities Are Also Listed

M	q	electronic configuration of HOMO	electron affinity (eV)
Sc	0	$(3de_{2g})^3$, $(4sa_{1g})^0$, $(3de_{1g})^0$, $(3da_{1g})^0$	
Sc	−1	$(3de_{2g})^4$, $(4sa_{1g})^0$, $(3de_{1g})^0$, $(3da_{1g})^0$	−0.73
Ti	0	$(3de_{2g})^4$, $(4sa_{1g})^0$, $(3de_{1g})^0$, $(3da_{1g})^0$	
Ti	−1	$(3de_{2g})^4$, $(4sa_{1g})^1$, $(3de_{1g})^0$, $(3da_{1g})^0$	−0.37
V	0	$(3de_{2g})^4$, $(4sa_{1g})^1$, $(3de_{1g})^0$, $(3da_{1g})^0$	
V	−1	$(3de_{2g})^4$, $(4sa_{1g})^2$, $(3de_{1g})^0$, $(3da_{1g})^0$	−0.29
Cr	0	$(3de_{2g})^4$, $(4sa_{1g})^2$, $(3de_{1g})^0$, $(3da_{1g})^0$	
Cr	−1	$(3de_{2g})^4$, $(4sa_{1g})^2$, $(3de_{1g})^1$, $(3da_{1g})^0$	0.12
Mn	0	$(3de_{2g})^4$, $(4sa_{1g})^2$, $(3de_{1g})^1$, $(3da_{1g})^0$	
Mn	−1	$(3de_{2g})^4$, $(4sa_{1g})^2$, $(3de_{1g})^2$, $(3da_{1g})^0$	0.10
Fe	0	$(3de_{2g})^4$, $(4sa_{1g})^2$, $(3de_{1g})^2$, $(3da_{1g})^0$	
Fe	−1	$(3de_{2g})^4$, $(4sa_{1g})^2$, $(3de_{1g})^2$, $(e_{2u})^1$, $(3d_{a1g})^0$	0.60
Co	0	$(3de_{2g})^4$, $(4sa_{1g})^2$, $(3de_{1g})^3$, $(3da_{1g})^0$	
Co	−1	$(3de_{2g})^4$, $(4sa_{1g})^2$, $(3de_{1g})^4$, $(e_{2u})^0$, $(3da_{1g})^0$	0.55
Ni	0	$(3de_{2g})^4$, $(4sa_{1g})^2$, $(3de_{1g})^4$, $(3da_{1g})^0$	
Ni	−1	$(3de_{2g})^4$, $(4sa_{1g})^2$, $(3de_{1g})^4$, $(e_{2u})^1$, $(3da_{1g})^0$	0.88

The electron affinity of $M(Bz)_2$ complexes plotted in Figure 8c shows a pattern almost opposite to that of MBz complex. Here we find that the electron affinity of $M(Bz)_2$ for M = Sc, Ti, V are negative and steadily increase toward Ni with a zigzag pattern.

The negative value of electron affinities of Sc, Ti, and V can be explained in terms of filling of the bonding orbitals $3de_{2g}$ and $4sa_{1g}$ (see Table 5). Electron affinity values become positive when filling of antibonding orbitals starts to occur in these complexes. In fact, the strong-field character of these complexes makes the $3da_{1g}$ orbital to be higher in energy than the e_{2u} combination of the $2e_{2u}$ unoccupied antibonding orbitals of the two benzenes. The order of magnitude of the electron affinities is clearly related to the energies of the orbitals being occupied: −0.73 eV when it is $3de_{2g}$ (Sc), ∼−0.3 when it is $4sa_{1g}$ (Ti, V), ∼0.1 eV when it is an unpaired $3de_{1g}$ orbital (Cr, Mn), and ∼0.6 eV when it is a paired $3de_{1g}$ or the benzene e_{2u} orbital (Fe, Co). The high value of the Ni complex may be attributed to the extra stabilization of the singlet, closed-shell configuration of the neutral species.

We are not aware of any systematic measurements of the electron affinities of the $M(Bz)_2$ metal system except for $V(Bz)_2$. Kaya and co-workers[17] have determined this electron affinity to be negative which is in agreement with our calculation. The negative electron affinity of $V(Bz)_2$ was also suggested earlier by electrochemical study.[40] What we find to be potentially interesting is that the electron affinity of $Ni(Bz)_2$ is 0.88 eV, while that of NiBz is −0.47 eV. Experimental confirmation of this prediction would be quite interesting.

IV. V− and Fe−Multidecker-Benzene Complexes

In this section we discuss the structure, relative stability, ionization potential, and magnetic properties of $V_2(Bz)_3$ and $Fe_2(Bz)_3$ complexes. In bulk, V is nonmagnetic, while Fe is ferromagnetic. In small clusters both V and Fe are ferromagnetic.

(40) While the paper was under review, we were able to obtain the fully optimized geometry of neutral $Ni(Bz)_2$ without any symmetry constraint. The resulting geometry revealed that, while the Ni atom sits on top of one benzene at the C_{6v} configuration, the second benzene lying above the Ni atom is displaced from the center as well as tilted. The C−C bond of this displaced benzene lies on top of the Ni atom. The energy gained in this configuration over that with D_{6h} symmetry is 1.22 eV. These results along with others involving multiple Ni atoms and benzene molecules without any symmetry constraint will be published later.

(41) Elschenbroich, C.; Bilger, E.; Metz, B. *Organometallics* **1991**, *10*, 2923.

Table 6. Dissociation Energy (eV) and Ionization Potential of $V_n(Bz)_{n+1}$ and $Fe_n(Bz)_{n+1}$ ($n \leq 2$) Complexes

	D_e0(eV)		D_e^+(eV)		I.P.(eV)	
	theo.	expt.	theo.	expt.	theo.	expt.
$V_1(Bz)_2$	3.57	3.19	2.63	2.42	6.05	5.75
$V_2(Bz)_3$	1.43	-	2.92	-	4.85	4.70
$Fe_1(Bz)_2$	1.09	-	3.28	2.15	5.06	5.18
$Fe_2(Bz)_3$	0.55	-	1.34	-	4.26	-

Our motivation for this study was not only to see if multidecker structures (see Figure 1) could explain the observed properties of V− and Fe−benzene complexes but also to determine if the metal atoms are magnetically coupled. We recall that the peaks in the mass spectra of V_nBz_m complexes correspond to $m = n + 1$. In case of Fe_nBz_m complexes the two major peaks are at $(n,m) = (1,2)$ and $(2,3)$, while the peaks at $(n,m) = (3,3)$, $(4,3)$, $(5,3)$, and $(6,4)$ have much reduced intensities. To optimize the structure of $M_2(Bz)_3$ (M = V, Fe) complexes, we have again used D_{6h} symmetry, frozen the structure and bond lengths of benzene, and allowed only metal atom−benzene distances to vary.

The distances of V and Fe to the nearest benzene plane in neutral $M_2(Bz)_3$ complexes are 1.70 and 1.74 Å, respectively. Note that they are significantly different from those in MBz complexes given in Figure 4 but are similar to those in $M(Bz)_2$. The relative stability of the $M_n(Bz)_{n+1}$ can be evaluated by computing the energy, D_e needed to dissociate this complex into $M_{n-1}(Bz)_n$ + MBz fragments. We define this energy as,

$$D_e[M_n(Bz)_{n+1}] = -\{E[M_{n-1}(Bz)_n] + E[MBz]\}$$

The results of the dissociation energies of neutral and charged states of $M_2(Bz)_3$ are presented in Table 6 and compared with smaller complexes. Note that the dissociation energies of neutral $V_1(Bz)_2$ and $Fe_1(Bz)_2$ are about a factor of 2 larger than those of $V_2(Bz)_3$ and $Fe_2(Bz)_3$, respectively. This indicates that the $M(Bz)_2$ is far more stable than the larger complexes. This is consistent with the mass spectra of M_nBz_m where the peaks corresponding to $(n,m) = (1,2)$ are the most prominent irrespective of what metal atom M stands for in the 3d series.

The ground states of the $V_2(Bz)_3$ and $Fe_2(Bz)_3$ optimized with the D_{6h} symmetry were found to be a singlet, that is, total spin = 0. With this symmetry constraint, the two metal atoms are equivalent, and thus, for a spin-singlet configuration, the net spin on each metal atom would be zero. That, indeed, turned out to be the case from a Mulliken analysis of the charge associated with majority and minority states. While such a situation could be imagined to hold for the V-system, it is difficult to imagine how the magnetic moments of Fe (which is ferromagnetic in the bulk) could be completely quenched to yield zero net spin at each Fe site. We, therefore, carried out the calculations with the C_1 symmetry that enables each metal atom to be different. Upon energy minimization, we, indeed, found both V and Fe atoms in $V_2(Bz)_3$ ad $Fe_2(Bz)_3$ to be antiferromagnetically coupled with a net moment of about $1\mu_B$ at each metal atom site in $V_2(Bz)_3$ and $2\mu_B$ in $Fe_2(Bz)_3$. Note that the total spin of the antiferromagnetic $V_2(Bz)_3$ and $Fe_2(Bz)_3$ is still zero. The antiferromagnetic configuration of $V_2(Bz)_3$ and $Fe_2(Bz)_3$ lies 0.29 and 0.27 eV, respectively, below their corresponding nonmagnetic states. The spin-triplet state of $Fe_2(Bz)_3$ lies 0.46 eV above antiferromagnetic ground state.

As indicated earlier, the only theoretical study of multidecker complexes that we are aware of was carried out by Weis et al.[20] on $V_n(Bz)_m^+$ system. Our calculated spin multiplicity of 4 for the $V_2(Bz)_3^+$ system is in agreement with the results of Weis et al.

The dissociation energies of $M_2(Bz)_3^+$ for M = V and Fe are not available for comparison with our theory. We note from Table 6 that while $D_e^+(V_2(Bz)_3^+)$ is slightly larger than that of $V(Bz)_2^+$, the dissociation energy of $Fe_2(Bz)_3^+$ is more than a factor two smaller than that of $Fe(Bz)_2^+$. The ionization potentials of $V_n(Bz)_{n+1}$ and $Fe_n(Bz)_{n+1}$ ($n \leq 2$) decreases steadily with increasing n, and the results agree very well with experiment.[22]

V. Conclusions

First-principles self-consistent calculations based on generalized gradient approximations to density functional theory were carried out to study the equilibrium geometries, energetics, electronic structure, and properties of 3d transition metal−benzene complexes containing up to two metal atoms and three benzene molecules. The results varied substantially from metal−benzene to metal−$(benzene)_2$ to $(metal)_2$−$(benzene)_3$ complexes. These variations were shown to be linked to the character of the highest occupied molecular orbitals. Following is a summary of our results.

(1) The bond lengths between carbon−carbon and carbon−hydrogen as well as the angle between the C−C and C−H bonds remain virtually unaffected in M−Bz complexes.

(2) The structure of MBz complexes have C_{6v} symmetry. While multiple $V_n(Bz)_{n+1}$ complexes do have the sandwich structure, indications are that such complexes involving Co and Ni may prefer an alternate structure. The distances of the metal atoms from the benzene plane depend not only on the atomic number of the metal elements but also on the net charge of the metal−benzene complex. In addition the variation of the metal−benzene distance across the 3d series is different between MBz and $M(Bz)_2$ complexes.

(3) The ionization potentials of MBz complex across the 3d series show the same trend as the transition metal atoms, but those of $M(Bz)_2$ are qualitatively different. While the ionization potentials in Sc−, Ti−, V−, Cr−Bz complexes are nearly constant, they rise from Sc to V before declining in $M(Bz)_2$ system. In particular, the ionization potential rises sharply from Cr to Mn in MBz, while it drops precipitously from Cr to Mn in $M(Bz)_2$.

(4) The dissociation energies of MBz complexes exhibit a minimum at Cr and rise as one moves away in either direction of the 3d series. This variation is intimately linked to the energy needed to flip the spin of the s electron in $3d^{n+1}\,4s^1$ configuration of the transition metal systems. The behavior is very different in $M(Bz)_2$ where the dissociation energies decrease from Ti to Ni. These trends in either MBz and $M(Bz)_2$ complexes persist when they exist in the cationic form. What we found to be the most interesting are special situations in $Cr(Bz)_2$, $Mn(Bz)_2^+$, and $V(Bz)_2^-$. While $Cr(Bz)_2$ and $Mn(Bz)_2^+$ are far more stable than Cr(Bz) and $Mn(Bz)^+$, respectively, $V(Bz)_2^-$ is unstable against autodetachment of the extra electron. Note that all of these systems contain 18-valence electrons each and should behave in a similar fashion.

(5) The electron affinity of the MBz complexes shows a pattern which is opposite to that of the metal atoms, M. For example, the electron affinity of free 3d atoms decreases from Sc to Ti, increases from Ti to Cr, decreases sharply from Cr to Mn, and increases from Mn to Ni. In MBz complexes, the electron affinity increases from Sc to Ti, decreases from Ti to Cr, increases slightly from Cr to Mn, and then declines toward Ni with $NiBz^-$ being unstable against autodetachment of the extra electron. In $M(Bz)_2$ complexes, the electron affinities increase steadily from Sc to Ni with small oscillatory change. In particular, Sc, Ti, and V systems are unstable against autodetachment. Results on VBz and $V(Bz)_2$ complexes agree with experiment.[22] No experimental information is available in any other systems.

(6) The spin multiplicities of M, MBz, and $M(Bz)_2$ systems are very different from each other. While the 3d metal atoms possess high-spin states in keeping with the Hund's rule, the preferred spins of M(Bz) complexes are governed by the Pauli principle: The spin multiplicities of Sc−, Ti−, V−Bz systems are enhanced, while those of Mn−, Fe−, Co−, Ni−Bz systems are reduced from their values in the free metal atom. In $M(Bz)_2$ complexes, strong hybridization of the electron from the second benzene molecule with the d electrons of the metal atoms substantially quenches their magnetic moments and reduces them to the lowest possible value with only the exception of $Fe(Bz)_2$ which is a triplet. Similar differences in spin multiplicities also occur for charged metal−benzene complexes.

(7) The ionization potentials and dissociation energies of $V_2(Bz)_3$ and $Fe_2(Bz)_3$ are consistently lower than those for $V(Bz)_2$ and $Fe(Bz)_2$ with only the exception of $V_2(Bz)_3^+$. Its dissociation energy is slightly larger than that for $V(Bz)_2^+$. In addition, the coupling between V atoms in $V_2(Bz)_3$ and Fe atoms in $Fe_2(Bz)_3$ is antiferromagnetic.

The comprehensive theoretical analysis provided here agrees with almost all of the experimental data available to date on these systems and explains all the trends. We also provide results on electron affinities, spin multiplicities, dissociation energies, and ionization potentials on systems for which no experiment exists. We hope that our work will stimulate those measurements. The lack of a good agreement between theory and experiment on $Co(Bz)_2$ and $Ni(Bz)_2$ systems suggests that the structures may differ from the D_{6h} symmetry. The geometries of these systems are being globally optimized with no symmetry constraints, and the results will be published in due course.

Acknowledgment. This work was supported in part (B.K.R. and P.J.) by a Grant from the Department of Energy (DE-FG02-96ER45579). R.P. acknowledges the support of Molecular Simulations Inc, San Diego, and M.A.B. is indebted to the Spanish DGICyT for Grant PB96-0559.

JA0035452